Journal of Computational Physics **164,** 48–61 (2000)
doi:10.1006/jcph.2000.6564, available online at http://www.idealibrary.com on IDEAL®

Simulating Solid Colloidal Particles Using the Lattice-Boltzmann Method

M. W. Heemels,* M. H. J. Hagen,† and C. P. Lowe*

**Computational Physics, Faculty of Applied Physics, Delft University of Technology, Lorentzweg 1, 2628 CJ Delft, The Netherlands; and †FOM Institute for Atomic and Molecular Physics, Kruislaan 407, 1098 SJ Amsterdam, The Netherlands*

Received January 20, 2000; revised June 12, 2000

The lattice-Boltzmann method is a technique for simulating the time-dependent motions of a simple fluid. Introducing rigid particles and imposing the correct boundary conditions at the solid/fluid interface allows the many-body, time-dependent hydrodynamic interactions between particles to be computed. Rather than simulating truly solid particles, a computationally convenient method for doing this uses hollow objects filled with the model fluid. We propose a simple modification of this "internal fluid" method. For computational convenience our method keeps the fluid inside the object. Its behaviour is modified, however, in such a way that it does not perturb the dynamics of the particle. The equations of motion for the solid particles are then modified in such a way that the microscopic conservation laws for mass and momentum are satisfied. Comparing both the time-dependent (rotational and translational) motion of an isolated spherical particle and the viscosity of a concentrated suspension of hard spheres against known results for solid particles, we examine artifacts attributable to the "internal" fluid. Using our modified approach, we show that these artifacts are no longer present and the behaviour of truly solid particles is recovered.

Key Words: colloidal suspensions; computer simulations; hydrodynamic interactions.

1. INTRODUCTION

The lattice-Boltzmann method is a simple scheme for simulating the dynamics of Newtonian fluids. By incorporating solid particles into the model fluid and imposing the correct boundary condition at the solid/fluid interface, one can use the method to study colloidal suspensions [1, 2]. Colloidal systems consist of particles that are large by molecular standards, dispersed in a solvent. Because of their ubiquity in both nature and in industry, we would like to be able to predict theoretically, or calculate numerically, their properties.

0021-9991/00 $35.00

Unfortunately, the complex nature of the hydrodynamic interactions between the particles makes this difficult. In the hybrid lattice-Boltzmann/solid-particle model, the hydrodynamic interactions governing the motion of the particles emerge quite naturally from the dynamics of the model fluid. As such, this model represents a useful numerical tool for studying suspensions. In this respect it has two particular strengths, both related to the fact that the velocity fields in the fluid evolve with the correct time dependence, i.e., it avoids the approximation of pseudo steady states. First, the technique can be used to probe the time-dependent nature of the interactions between the particles [3, 4]. Second, it can be used to study the effects of inertia on suspensions [5]. Particulate flows for which the Reynolds number is not negligible can be simulated. Inertia is important if, for example, the particles are large ($\gg 1\,\mu$) or the suspension is very far from equilibrium (which is commonly the case during processing).

The essentials of simulating colloidal suspension within the lattice-Boltzmann framework were derived by Ladd [1]. Here we will just recapitulate the most important points. The lattice-Boltzmann method models a compressible fluid (in which the speed of sound is finite). It is based on solving Boltzmann's equation for particles constrained to move on a lattice (see, for example, Ref. [6]). The state of the fluid system is characterized by the single-particle distribution function $n_i(\mathbf{r}, t)$, describing the average number of particles at a particular node of the lattice $\mathbf{r}$, at a time t, with the discrete velocity $\mathbf{c}_i$. The hydrodynamic fields, mass density ρ, momentum density $\mathbf{j}$, and the momentum flux density $\mathbf{\Pi}$ are simply moments of this velocity distribution:

$$\rho = \sum_i n_i, \quad \mathbf{j} = \sum_i n_i \mathbf{c}_i, \quad \mathbf{\Pi} = \sum_i n_i \mathbf{c}_i \mathbf{c}_i. \tag{1}$$

A convenient lattice to use is the 4D face-centered hypecubic (FCHC) lattice. A two- or three-dimensional model, with sufficient symmetry to ensure that the hydrodynamic transport coefficients are isotropic, can be obtained by projection onto the number of required dimensions. The time evolution of the distribution functions n_i is described by the discretized analogue of the Boltzmann equation [7],

$$n_i(\mathbf{r} + \mathbf{c}_i, t + 1) = n_i(\mathbf{r}, t) + \Delta_i(\mathbf{r}, t), \tag{2}$$

where Δ_i is the change in n_i due to instantaneous "collisions" at the lattice nodes. The post-collision distribution $n_i + \Delta_i$ is propagated in the direction of the velocity vector $\mathbf{c}_i$. A complete description of the collision process is given in [1]. The main effect of the collision operator $\Delta_i(\mathbf{r}, t)$ is to (partially) relax the shear stress at every lattice site. The rate of stress relaxation, or equivalently, the kinematic viscosity ν, can be chosen almost freely.

The motion of the colloidal particle is determined by the force and torque exerted on it by the fluid. These are in turn a result of the stick boundary conditions applied at the solid/fluid interface (that the fluid velocity and surface velocity are equal). For a stationary boundary a simple bounce-back rule performed on boundary links enforces the stick boundary condition. Boundary links are links connecting lattice sites inside and outside the solid object, and obviously these come in pairs. We adopt a convention of labelling the link which goes from inside to outside as ib and its partner as $-ib$. For a moving boundary the bounce-back rule is still applied but some of the particles moving in the same direction as the solid object are allowed to "leak" through, matching the fluid velocity to the object

velocity at the boundary. Note that this requires there to be fluid both inside and outside the particle. For the lattice-Boltzmann model the modified bounce-back rule takes the form [1]

$$\begin{aligned} n_{-ib}(\mathbf{r}_b) &= n_{ib}(\mathbf{r}_b) - 4n_0(\rho)\mathbf{u}_b \cdot \mathbf{c}_{ib} \\ n_{ib}(\mathbf{r}_b) &= n_{-ib}(\mathbf{r}_b) + 4n_0(\rho)\mathbf{u}_b \cdot \mathbf{c}_{ib}, \end{aligned} \tag{3}$$

where $n_0(\rho)$ is the zero velocity distribution and $\mathbf{u}_b$ is the *local* boundary velocity. For a colloidal particle with linear and angular velocities of $\mathbf{u}_o$ and ω_o respectively, the local boundary velocity is just

$$\mathbf{u}_b = \mathbf{u}_o(t) + \omega_o(t) \times \mathbf{r}_b, \tag{4}$$

where $\mathbf{r}_b$ is the vector connecting the centre of mass of the object to the midpoint of the boundary link. The force $\mathbf{F}$ and torque $\mathbf{T}$ exerted by the fluid on the particle are computed from the change in momentum of the fluid as a result of the boundary collisions. The force at each individual boundary link, $\mathbf{F}_{ib}(\mathbf{r}_b)$, is given by

$$\mathbf{F}_{ib}(\mathbf{r}_b) = 2(n_{ib}(\mathbf{r}_b) - n_{-ib}(\mathbf{r}_b) - 4n_0(\rho)\mathbf{u}_b \cdot \mathbf{c}_{ib})\mathbf{c}_{ib}. \tag{5}$$

The total force and torque acting on the object are calculated by summing these link forces, together with any external forces ($\mathbf{F}_x$) or torques ($\mathbf{T}_x$), giving

$$\begin{aligned} \mathbf{F} &= \sum_{ib} \mathbf{F}_{ib}(\mathbf{r}_b) + \mathbf{F}_x \\ \mathbf{T} &= \sum_{ib} \mathbf{F}_{ib}(\mathbf{r}_b) \times \mathbf{r}_b + \mathbf{T}_x. \end{aligned} \tag{6}$$

Having determined the force and torque acting on an object we are now in a position to solve the equations of motion. There are several methods for doing this [1, 5, 8]. We prefer the "self-consistent" method described in Ref. [8]. It provides unconditional stability without the necessity of introducing, in addition to the time step used to integrate the Boltzmann equation, a second, smaller, time step over which to integrate the equations of motion. This method involves rewriting Eq. (4) in terms of the new object velocities (indicated by a prime)

$$\mathbf{u}_b = \mathbf{u}'_o + \omega'_o \times \mathbf{r}_b \tag{7}$$

and then substituting the modified expression for $\mathbf{u}_b$ into the discretized equations of motion. We can solve the resulting equations for the α component of $\mathbf{u}'_o$ and ω'_o, giving

$$u'_{o\alpha} = \frac{F_{x\alpha}/m_o + m_o u_{o\alpha}(t) + 2\sum_{ib}(n_{ib}(\mathbf{r}_b) - n_{-ib}(\mathbf{r}_b))c_{ib\alpha}}{m_o + 8n_0(\rho)\sum_{ib} c_{ib\alpha}c_{ib\alpha}} \tag{8}$$

$$\omega'_{o\alpha} = \frac{T_{x\alpha}/I_o + I_o\omega_{o\alpha} + 2\sum_{ib}(n_{ib}(\mathbf{r}_b) - n_{-ib}(\mathbf{r}_b))(\mathbf{r}_b \times \mathbf{c}_{ib})_\alpha}{I_o + 8n_0(\rho)\sum_{ib}(\mathbf{r}_b \times \mathbf{c}_{ib})_\alpha(\mathbf{r}_b \times \mathbf{c}_{ib})_\alpha}. \tag{9}$$

Using this method, we find that the new fluid velocity at the boundary implies a force and torque on the object, which, when incorporated into the equations of motion of the object, imply the same new velocity for the particle—the rule is self-consistent.

In this article we address the following point. Because the approach outlined above requires fluid both inside and outside the object it cannot be regarded *a priori* as representing a truly solid particle. It actually describes the dynamics of a hollow shell, of mass m_o and moment of inertia I_0, filled with fluid. Now, it may be that the behaviour of these two systems is broadly similar, in which case the presence of the internal fluid is not problematic. Indeed, the method outlined above has been successfully applied in several studies. Ladd [2] investigated the influence of the internal fluid on the rotational dynamics of a single spherical particle and showed the following. For high-frequency rotational motion ($\Omega \gg \nu/a^2$, where Ω is the frequency, ν is the kinematic viscosity, and a is the particle radius) the internal fluid makes no contribution and the particle displays behaviour characteristic of a solid sphere with moment of inertia I_o. For low-frequency motion ($\Omega \ll \nu/a$) the internal fluid contributes essentially as a rigid body and the particle displays behaviour characteristic of a solid particle with an effective moment of inertia, I_o^*, comprising the moment of inertia of the shell and the moment of inertia of internal fluid; i.e., for a sphere

$$I_o^* = I_o + \sum_{\mathbf{r}_{\text{int}}} bn_o |\mathbf{r}_{\text{int}} - \mathbf{r}_0|^2, \tag{10}$$

where b is the number of discrete velocities ($b = 24$ for the FCHC lattice), $\mathbf{r}_0$ is the position vector for the centre of the sphere, and $\mathbf{r}_{\text{int}}$ are the position vectors of the N_{int} lattice nodes inside the object. By analogy, for translational motion we would expect a particle to behave as if it had a mass m_o at high frequencies but an effective mass $m_o^* = m_o + N_{\text{int}} bn_0$ at low frequencies. This is not particularly satisfactory because the ratio of the mass of a colloidal particle to the mass of the equivalent volume of fluid, ρ^*, is an important parameter determining the dynamics of a colloidal particle. It influences the inertial time scale for the colloidal particle (the characteristic time it takes the particle to respond to changes in the velocity of the fluid surrounding it). If one is interested in the effects of inertia it would be preferable to get this right. Furthermore, the parameter ρ^* does not vary much in real suspensions. It always takes a value close to unity, otherwise the particles would separate out under the effects of gravity. If we try to simulate a neutrally buoyant particle ($\rho^* = 1$) using the above approach, at best we can choose between setting $m_o = 0$ and having the correct low-frequency behaviour or setting $m_o = N_{\text{int}} bn_0$ and having the correct high-frequency behaviour.

Given the above, it is not surprising that attempts have been made to develop a scheme for simulating colloidal particles that does not involve internal fluid [5, 9, 10]. To our knowledge, none of these methods are completely satisfactory in that they do not conserve both mass and momentum. There is also the question of whether we actually want to get rid of the internal fluid or keep it and get rid of its contribution to the effective particle mass and moment of inertia. Dispensing with it altogether actually creates a new problem. That is, as the particle moves over the lattice some nodes that were external become internal and vice versa. If the nodes inside the particle are undefined (i.e., there is no internal fluid) we then face problems. In particular, how do we define the state of an "exposed" node, i.e., a node that was inside the particle but suddenly becomes part of the system [5]? Taking this into consideration, the second of the two options, keeping the internal fluid but mitigating its effects, is probably preferable as it limits these problems. In the following sections we describe and test such a method.

2. REMOVING THE EFFECTS OF THE INTERNAL FLUID

The method we propose to minimize the effects of the internal fluid and the reasoning behind it proceed along the following lines. Suppose the internal fluid is at rest. In this case it is straightforward to see that, if we use the original method outlined above, the internal fluid summed over the entire object no longer contributes a variable net force or torque. Consequently it does not enter into the equations of motion. Making use of this fact, we therefore adopt a two-stage process. The first stage is to impose the condition that the internal fluid remains at rest. To this end, at the start of each time step we reset all the distribution functions inside a particle $n_i(\mathbf{r}_{\text{int}}, t)$ to values characteristics of a fluid at rest, i.e.,

$$n_i(\mathbf{r}_{\text{int}}, t)' = \frac{\sum_{\mathbf{r}_{\text{int}}} \sum_i n_i(\mathbf{r}, t)}{bN_{\text{int}}}. \tag{11}$$

The value of this constant ensures conservation of mass (all mass inside the particle is equally redistributed, thus dissipating any sound propagation within the particle). This step does not conserve linear or angular momentum. However, if the changes of linear and angular momentum, resulting from step 1, are interpreted as inducing an external force and torque on the particle,

$$\begin{aligned} \mathbf{F}_x &= -\sum_{\mathbf{r}_{\text{int}}} \sum_{\mathbf{c}_i} (n_i(\mathbf{r}_{\text{int}}, t)' - n_i(\mathbf{r}_{\text{int}}, t))\mathbf{c}_i \\ \mathbf{T}_x &= -\sum_{\mathbf{r}_{\text{int}}} \sum_{\mathbf{c}_i} (n_i(\mathbf{r}_{\text{int}}, t)' - n_i(\mathbf{r}_{\text{int}}, t))(\mathbf{r} - \mathbf{r}_o) \times \mathbf{c}_i, \end{aligned} \tag{12}$$

then, when these forces and torques are substituted into the equations of motion (Eqs. (8) and (9)) and the state of the system is updated from $t \to t + \Delta t$ in the usual manner, both linear and angular momentum are conserved over the full time step. At the end of this second step, the internal fluid adjacent to the shell of the particle will generally not be at rest (because of the intervening boundary collisions). However, we will now apply the first operation again. This can therefore be interpreted as transferring the momentum that would, using the original method, have been transferred into the internal fluid back to the shell—where it belongs. In essence, we preserve Ladd's original method for imposing the stick boundary condition but apply a small correction preventing momentum transfer to the interior fluid. The internal fluid thus acquires no linear or angular momentum and does not contribute to the equations of motion.

If we consider a colloidal particle that is moving from one lattice site to another, the method we outlined above, because it keeps the internal fluid, possibly provides a convenient point at which to perform the move. This point is probably prior to the application of the first operation. The reason for this is the following. The normal bounce-back rule (step two) applies the stick boundary condition to both the exterior and interior of the solid/fluid interface. Thus, at this point in the algorithm, nodes adjacent to the boundary, both inside and outside, will be set to the correct velocity. Therefore, if a particle moves and a node originally inside the object is now outside, it will, to a good approximation, be in the correct state. Using the method outlined above we can deal with a particle moving over the lattice by nodes that are already identified. This is in contrast to approaches which remove the internal fluid completely [5].

3. TESTS OF THE METHOD

As a test of the method outlined above, we consider three different dynamic properties of colloidal systems. Our aim is to apply the original method, establish the role of the internal fluid, and then apply the new method for comparative purposes. Specifically we have calculated the following. First, we have the frequency-dependent rotational friction coefficient of an isolated colloidal sphere. This is the same problem considered by Ladd [2]. Second, we calculate the single-particle velocity autocorrelation function for a single colloidal sphere. In contrast to rotation, sound propagation (related to mass conservation) influences this quantity. Finally, we consider a transport property, the viscosity of a concentrated suspension of colloidal hard spheres. For the first two cases there is an analytic result with which to compare. For the third we can compare with accurate numerical values, calculated using multipole methods [12], or theory, valid at low to intermediate volume fractions. In all the simulations we report here, the shell mass and moment of inertia (m_o and I_o) are set to values characteristic of a solid sphere with the same density as the density of the fluid. Thus, if the effects of the internal fluid can be neglected, we are simulating neutrally buoyant particles.

3.1. *The Frequency-Dependent Rotational Friction Coefficient*

If we consider one Fourier component of the velocity of a particle executing some arbitrary time-dependent rotational motion, i.e., $\omega_o(t) = \Omega_0 \cos(\Omega t)$, then the fluid will exert a frequency-dependent torque $T_f(\Omega)$ on the particle with the general form

$$T_f(\Omega) = \Omega_0 \gamma_r(\Omega), \tag{13}$$

where $\gamma_r(\Omega)$ is a frequency-dependent rotational friction coefficient. The time-dependent motion of a single spherical particle can be analyzed theoretically in considerable detail. By assuming that the dynamics of the fluid can be described by the Navier–Stokes equations for an incompressible fluid (in the limit of zero Reynolds number) and that a stick boundary condition applies at the solid/fluid interface, this problem can be solved [11] analytically. For a particle of radius a suspended in a fluid of viscosity η and density ρ the result is

$$\gamma_r(\Omega) = -\gamma_0 \left(1 - \frac{i\Omega^*}{3(1+\sqrt{-i\Omega^*})} \right), \tag{14}$$

where $\nu = \eta/\rho$ is the kinematic viscosity, $\Omega^* = \Omega a^2/\nu$, and $\gamma_r(0)$ $(=8\pi\eta a^3)$ is the zero-frequency rotational friction coefficient. If the spherical particle is not solid but filled with fluid, there is an additional contribution to the friction coefficient coming from the internal fluid $\gamma_R^{\text{int}}(\Omega)$. At low values of the reduced frequency, $\Omega^* \ll 1$, this contribution takes the form

$$\gamma_R^{\text{int}}(\Omega) = \frac{\gamma_r(0)}{15} \Omega^* \left(i - \frac{\Omega^*}{35} \right). \tag{15}$$

The first term represents the inertial contribution of the internal fluid acting as a rigid body. Numerically, it is straightforward to calculate $\gamma_R(\Omega)$. We simply impose a sinusoidal velocity on the particle and calculate the in-phase and out-of-phase components of the torque exerted on the particle by the fluid. These are conveniently expressed in terms of a magnitude and phase shift. We concentrate here on low frequencies, where the effect of the internal fluid is

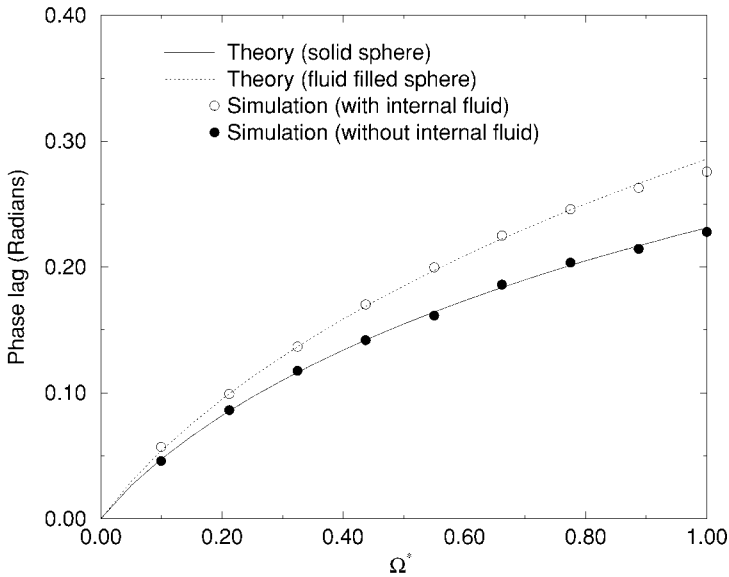

FIG. 1. Phase lag (in radians) between an imposed sinusoidal rotation with frequency Ω and the torque exerted on a colloidal sphere. The lag is plotted as a function of dimensionless frequency $\Omega^* = \Omega a^2/\nu$.

discernible but numerical errors (due to the discretization in time) remain small [2]. At low frequencies the effect of the internal fluid on the magnitude is slight. The dominant effect is an additional contribution to the phase shift (Eq. (15)). The results we obtained, using a sphere of radius 4.5 lattice spacings, are plotted in Fig. 1, along with the analytical result for a solid sphere (Eq. (14)) and the asymptotic result for a fluid-filled sphere (for which the rotational friction coefficient is simply the sum of the internal and external contributions). The simulations were carried out using both the original method described by Ladd [1] ("with internal fluid") and the modified method outlined above (denoted "without internal fluid"). As Fig. 1 shows, for the simulations using the original algorithm the inertial contribution at low frequencies is clearly visible. Just as Ladd concluded [2], at low frequencies the particle behaves like a solid sphere with a moment of inertia equal to that of the shell plus that of the equivalent volume of fluid. In contrast, using the modified method we described above, there is no additional inertial contribution. The data follow the theoretical curve for a solid object with a moment of inertia simply equal to the assigned moment of inertia I_o. Thus, from the point of view of rotation, the method we outlined above succeeds in its objective of removing the low-frequency effects of the internal fluid.

3.2. *The Single-Particle Velocity Autocorrelation Function*

We now turn to translational motion, where, this time, we will consider a more physical quantity, the velocity autocorrelation function (VACF). In a suspension a colloidal particle experiences rapid collisions with the solvent molecule, giving it a fluctuating thermal velocity. The VACF, $C(t)$, is defined as an average over these fluctuations $C(t) = \langle v(0)v(t)\rangle$, where $v(t)$ is one component of the instantaneous thermal velocity. It characterizes the decay of velocity fluctuations. In our lattice-Boltzmann model we have no spontaneous fluctuations. However, if we impose a velocity fluctuation then, according to Onsager's regression hypothesis, the subsequent decay will be identical to the average decay in a real

system. To analyze the dissipation of an imposed velocity fluctuation, in the same way that we defined a rotational friction coefficient above, we define a translational frequency-dependent friction coefficient $\gamma_t(\Omega)$. The translational friction coefficient characterizes the force acting on a particle undergoing simple periodic translational motion with frequency Ω. Since the function $\gamma_t(\Omega)$ connects the velocity to its derivative, it can be used to define an equation of motion for the particle. In terms of Fourier components, the velocity of the particle satisfies the equation

$$v(\Omega) = \frac{F_x(\Omega)/m_o}{-i\Omega + \gamma_t(\Omega)/m_o}, \tag{16}$$

where $F_x(\Omega)$ is the Fourier transform of any time-dependent external forces acting on the particle. If we now consider a particle impulsively accelerated to a velocity v_o at $t = 0$, i.e., $F_x(\Omega) = m_o v_0$, then

$$\frac{v(\Omega)}{v_0} = \frac{1}{-i\Omega + \gamma_t(\Omega)/m_o}. \tag{17}$$

Following from the discussion above, this can be related to the Fourier transform of the "true" VACF,

$$\frac{v(\Omega)}{v_0} = \frac{C(\Omega)}{C(t=0)} = \frac{m_o C(\Omega)}{k_B T}, \tag{18}$$

where T is the temperature and k_B is Boltzmann's constant. We have also used the equipartition condition to identify $C(t = 0) = k_B T/m_o$. So, if we know $\gamma_t(\Omega)$ then, with the aid of Eq. (17), Eq. (18), and an inverse transformation, we can calculate the velocity autocorrelation function. For a single spherical particle $\gamma_t(\Omega)$ can be calculated analytically. Assuming that the motion of the fluid is described by the compressible Navier–Stokes equations and that a stick boundary condition applies at the solid/fluid interface, this calculation yields [13, 14]

$$\gamma_t(\Omega) = 2\gamma_t(0)\alpha^2 \frac{(1+\alpha+(1/9)\alpha^2)B - (1/9)\beta^2 A}{\beta^2 A + 2\alpha^2 B}, \tag{19}$$

with

$$\begin{aligned} A &= 1 + \alpha + \frac{1}{3}\alpha^2 \\ B &= 1 + \beta + \frac{1}{3}\beta \\ \alpha &= -ia\sqrt{\Omega/\nu} \\ \beta &= \frac{ia\Omega}{\sqrt{(c^2 - i\Omega((4/3)\nu + \nu_B))}} \end{aligned} \tag{20}$$

Here $\gamma_t(0) = 6\pi\eta a$ is the zero-frequency translational friction coefficient, $\nu_B = \eta_B/\rho$, where η_B is the bulk viscosity, and c is the speed of sound through the fluid. The latter two quantities are associated with, respectively, the speed and the rate of damping of the sound wave generated by a moving particle. Comparisons have been made between theoretical and numerical values, calculated using the lattice-Boltzmann model [2], for the VACF

of a single spherical colloidal particle. However, the comparison was made against theory derived using the additional assumption that the fluid is incompressible (the compressible result, Eq. (19), reduces to the incompressible result in the limit $\beta \to 0$, i.e., the speed of sound going to infinity). The lattice-Boltzmann approach simulates a compressible system; the sound propagates through the model fluid at a finite speed. Although the effects of compressibility are limited to high frequencies, $\Omega \sim c/a$ [14], a comparison with the full compressible result, notably at short times, is more appropriate.

Numerically, we have calculated the normalized velocity autocorrelation function along the lines outlined above (Eq. (18)). Starting with a fluid at rest and a spherical particle with a velocity v_0, we allowed the system to evolve in time and, from the subsequent velocity of the particle, $v(t)$, we calculated the normalized velocity autocorrelation function $v(t)/v_0$. We performed the same procedure for particle radii of 2.5 and 4.5 lattice sites using a cubic system with periodic boundary conditions applied at the faces of the simulation box. We only calculated the VACF up until times less than the time it takes a sound wave to pass between the central particle and its nearest periodic image. Thus, the results are free from any finite size effects. In Fig. 2 we have plotted the normalized velocity autocorrelation function as a function of the viscous time $\tau_\nu = t\nu/a^2$ calculated using the original method and using the modified method outlined above. For the results plotted in Fig. 2 the radius of the solid particle was 2.5 lattice sites. Also plotted in Fig. 2 is the theoretical result for a compressible fluid, calculated by substituting appropriate values for the transport coefficients into Eq. (19) and transforming the frequency-dependent VACF into the time domain. In lattice units, such that the time step, density of the fluid, and lattice spacing are all unity, the values of the transport coefficients were $\nu = 1/6$, $c = 1/\sqrt{2}$, and $\nu_B = 1/30$. In Fig. 3 we show the same plot for data obtained using the identical fluid, but this time using a sphere of radius 4.5 lattice sites. Examining Fig. 2 we see that the VACF calculated with

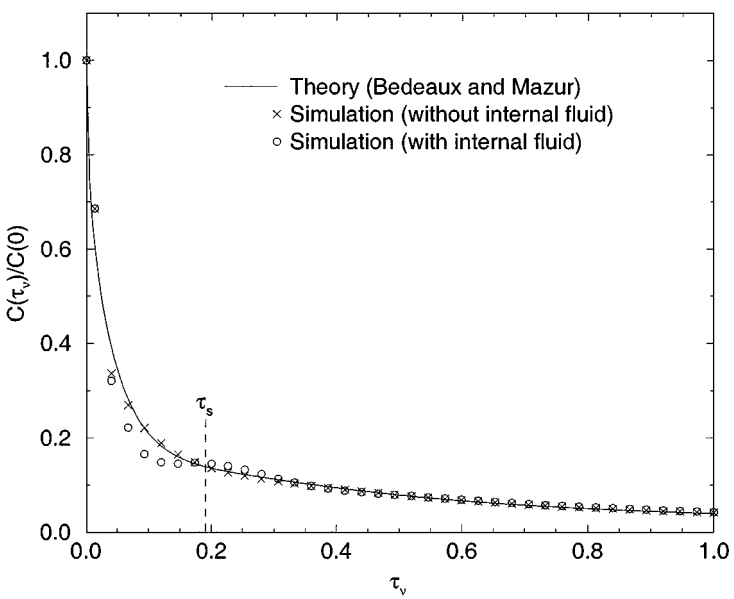

FIG. 2. The normalized velocity autocorrelation function for a single colloidal sphere as a function of dimensionless time $\tau_\nu = t\nu/a^2$. τ_s is the time, measured in the same reduced units, it takes a sound wave to travel a particle diameter. The simulation used a particle of radius 2.5 lattice sites.

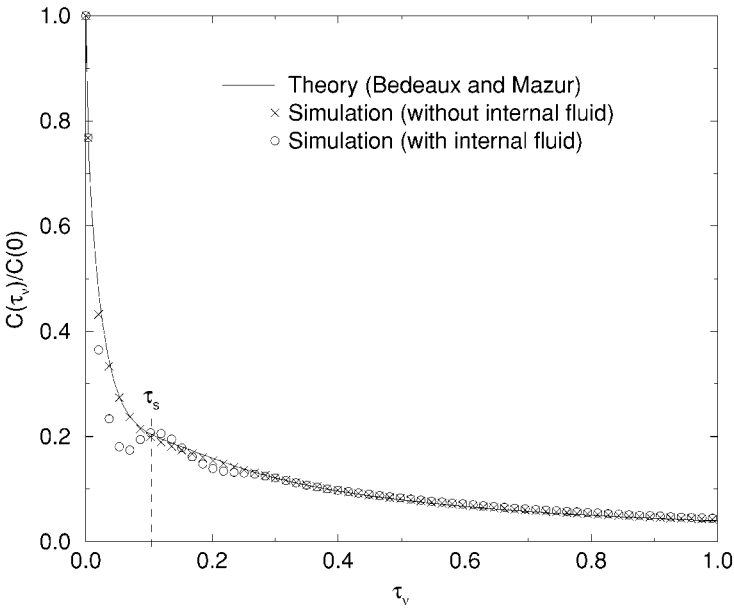

FIG. 3. The normalized velocity autocorrelation function for a single colloidal sphere as a function of dimensionless time $\tau_\nu = t\nu/a^2$. τ_s is the time, measured in the same reduced units, it takes a sound wave to travel a particle diameter. The simulation used a particle of radius 4.5 lattice sites.

the effects of the internal fluid removed ("without internal fluid") follows the theoretical curve and more closely than does the curve calculated using the original method. With the internal fluid present, the VACF lies initially below the theoretical curve and then subsequently above it. It displays weak oscillations about the true result. This is almost certainly an effect of sound propagating back and forth inside the object. To support this hypothesis, the time it takes a sound wave to travel one particle diameter is also shown in the plot (τ_s). As we can see, it corresponds to an artificial maximum in the VACF. Turning to the plot for the sphere of radius 4.5 lattice units (Fig. 3), we see that the oscillations about the correct result, for the simulation with internal fluid, are now, compared to the radius 2.5 case, more pronounced. Again the first artificial maximum occurs at a time commensurate with a sound wave travelling one diameter through the fluid (τ_s). This is consistent with our remark that these oscillations are an artifact of sound propagation through the internal fluid. Given that we are using a bigger representation of the sphere we should get a more accurate answer. The spatial resolution of the simulation has been increased. However, the artificial oscillations we observe are more pronounced. At short times we are further away from the true result. The reason for this is that, by moving from a sphere of radius 2.5 to 4.5, we have, in dimensionless terms decreased the compressibility. Sound waves are dissipated proportionately more slowly, making the problem worse. In contrast, for the simulation where we have attempted to remove the effects of the internal fluid, increasing the radius of the sphere gives a result nearer to the theoretical curve. This is the behaviour we would expect for a truly solid particle. On the whole, the agreement between the theoretical result and the simulations with the effects of the internal fluid removed is very good, particularly given the extremely rapid initial decay of the function relative to one time step. At longer times, after the oscillations induced by the internal fluid have died away, Figs. 2 and 3 suggest that either method is adequate. However, on closer examination we find that this

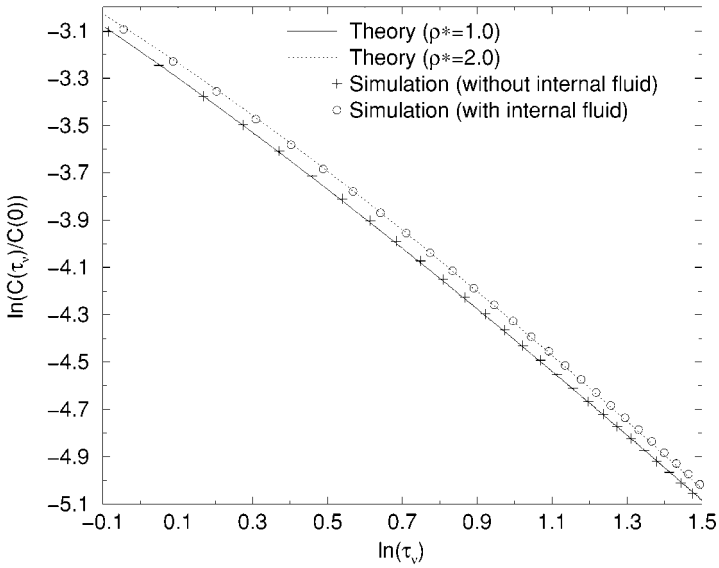

FIG. 4. Log–log plot of the normalized velocity autocorrelation function at longer dimensionless times, $\tau_v = t\nu/a^2$. The simulation used a particle of radius 2.5 lattice sites.

is not true. In Fig. 4 we have plotted, in log–log form, the decay of the VACF at longer times for a particle of radius 2.5. It is clear that, with the internal fluid present, the results follow the theoretical curve for a particle with mass ratio $\rho^* = 2$. Again, as with rotation, the internal fluid is contributing, at low frequencies (or in this case long times), a rigid-body inertial term to the equations of motion. In contrast, if we use the approach outlined above, the results follow the (correct) curve for a neutrally buoyant particle. Again our method seems to successfully reproduce the dynamics of a solid particle.

3.3. *The Viscosity of a Concentrated Suspension*

Whereas for generalized rotational and translational motion, considered above, the internal fluid causes a relatively minor perturbation of the dynamics of the particle, we now turn to what may be a more serious problem: the influence this may, in turn, have on the transport coefficients. Specifically, we consider the viscosity of a concentrated suspension. There are various ways to calculate this quantity. Probably the most convenient is by studying the decay of an initial transverse sinusoidal velocity perturbation [15] $v_{ix}(0) = \sin(kr_{iy})$, where $v_{ix}(0)$ is the x component of the velocity of particle i and r_{iy} is the y component of its position vector. If we calculate the subsequent velocity, $v_{ix}(t)$, of the N particles in the system, then according to classic hydrodynamics [16] we have

$$C_v(t) = \frac{1}{N}\left\langle \sum_{i=1}^{N} v_{ix}(0)v_{ix}(t) \right\rangle = \frac{1}{N}\left(\sum_{i=1}^{N} v_{ix}^2(0) \right) \exp(-k^2\nu_\phi t), \tag{21}$$

where the angular brackets denote an average over all possible configurations of the N particles and ν_ϕ is the kinematic viscosity of the suspension. We only expect Eq. (21) to apply on length scales long compared to the length scale defined by the particles themselves, i.e., $k \ll 2\pi/a$. The decay of this correlation function has been reported elsewhere [15];

here it is sufficient to note that the small-k asymptotic behaviour is observed, to a very good approximation, as long as $ka < 0.1$. The point is that this method gives us a means of determining the kinematic viscosity of the suspension. This is related to the suspension viscosity, η_ϕ, by $\eta_\phi = \rho\nu_\phi$, as long as we know the density. But what should we take for the density? If the particles are neutrally buoyant the density of a suspension, regardless of the volume fraction, will be equal to the density of the solvent, so that

$$\frac{\nu_\phi}{\nu} = \frac{\eta_\phi}{\eta}. \tag{22}$$

If, however, we set the shell mass so that the particles are nominally neutrally buoyant but the internal fluid contributes an equivalent mass (that is, assuming that it is the low-frequency particle mass that is relevant) then the density of the suspension ρ_ϕ, at volume fraction ϕ, will effectively differ from the solvent density as $\rho_\phi = (1+\phi)\rho$. This being the case, we then expect

$$\frac{\eta_\phi}{\eta} = \frac{(1+\phi)\nu_\phi}{\nu}. \tag{23}$$

Using the methodology outlined above (described in more detail in Ref. [15]), we have calculated the kinematic viscosity of a suspension of hard spheres as a function of volume fraction. In Fig. 5 we have plotted ν_ϕ/ν as a function of volume fraction for nominally neutrally buoyant particles, simulated using Ladd's original method ("with internal fluid") and using the modified method we outlined above ("without internal fluid"). Also plotted in Fig. 5 are theoretical predictions (based on an expansion up to second order in the volume

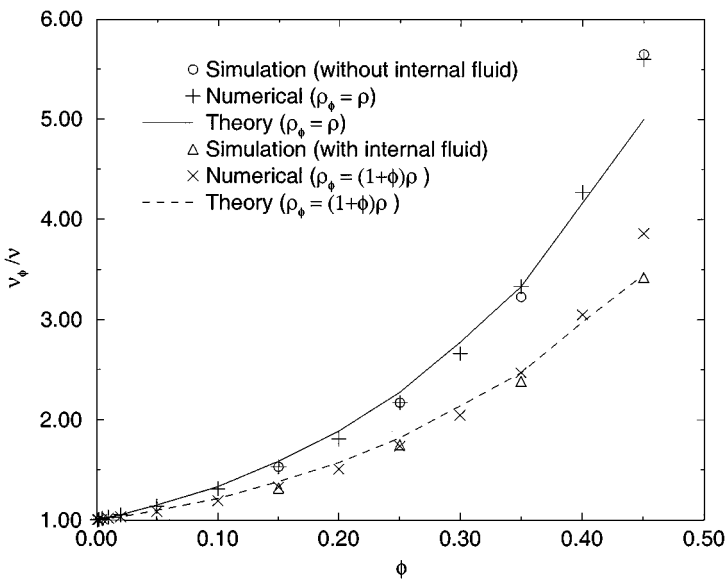

FIG. 5. The kinematic viscosity of a suspension of hard spheres, ν_ϕ, normalized by the solvent viscosity ν and plotted as a function of volume fraction ϕ. Data denoted "Numerical" refer to values derived from shear viscosities calculated by Ladd [12] and data denoted "Theory" refers to values derived from shear viscosities predicted by the theory of Beenakker and Mazur [17]. ρ_ϕ is the density we used to calculate the kinematic viscosity from the shear viscosity and ρ is the solvent density.

fraction [17]) for the kinematic viscosity of a suspension of neutrally buoyant particles and accurate numerical values calculated by Ladd [12]. As we see from the figure, whereas data calculated using the modified method agree with theoretical and numerical values for a suspension of neutrally buoyant particles, data calculated using the original method do not. The data clearly follow the curve $\nu_\phi/\nu = \eta_\phi/(1+\phi)\eta$. The internal fluid is therefore contributing to the effective density of the suspension (Eq. (23)) and the kinematic viscosity is increasingly underestimated with increasing volume fraction.

4. DISCUSSION

We have described a method for simulating truly solid colloidal particles within the lattice-Boltzmann framework. Unlike other methods that have been proposed, our method strictly adheres to the microscopic conservation laws for mass and momentum. For computational convenience our approach keeps the internal fluid inherent in Ladd's original model. However, by transferring linear and angular momentum that would otherwise have been transported to the internal fluid back to the shell of the particle, we recover the dynamics of a truly solid particle. We demonstrated this by showing that the correct time-dependent rotational and translation dynamics of a solid particle were recovered. To our knowledge, the theoretical result for the VACF of a colloidal particle suspended in a compressible fluid has not been tested before. Thus, our simulations could equally well be regarded as a test of the theory rather than vice versa. Either way, the agreement was excellent. For the simulations where the internal fluid reacted passively, we reached the same conclusion as Ladd. At low frequencies, or long times, the internal fluid contributes an additional rigid-body inertia to the motion of the particles. By considering the viscosity of a concentrated suspension, we showed that this additional inertia leads to a suspension with an effective density greater than one would expect for a suspension of colloidal particles with the same density of the fluid. This means that the kinematic viscosity and viscosity do not display the same dependence on volume fraction. Using our modified method, the correct equivalence was recovered.

ACKNOWLEDGMENTS

The research of Dr. Lowe has been made possible by a fellowship of the Royal Netherlands Academy of Arts and Sciences. We are indebted to Tony Ladd and Ignacio Pagonabarraga for their useful comments.

REFERENCES

1. A. J. C. Ladd, *J. Fluid Mech.* **271**, 285 (1994).
2. A. J. C. Ladd, *J. Fluid Mech.* **271**, 311 (1994).
3. A. J. C. Ladd, *Phys. Rev. Lett.* **70**, 1339 (1993).
4. C. P. Lowe and D. Frenkel, *Phys. Rev. E* **54**, 2704 (1996).
5. C. K. Aidun, Y. Lu, and E. J. Ding, *J. Fluid Mech.* **373**, 287 (1998).
6. G. R. McNamara and B. J. Alder, in *Microscopic Simulation of Complex Hydrodynamic Phenomena*, edited by M. Mareschal and B. L. Holian (Plenum, New York, 1992), p.
7. U. Frisch, D. d'Humières, B. Hasslacher, P. Lallemand, Y. Pomeau, and J.-P. Rivet, *Complex Syst.* **1**, 649 (1987).
8. C. P. Lowe, D. Frenkel, and A. J. Masters, *J. Chem. Phys.* **103**, 1582 (1995).

9. C. K. Aidun, Y. Lu, and E. J. Ding, *J. Stat. Phys.* **81**(1/2), 49 (1995).
10. D. Qi, *J. Fluid Mech.* **385**, 41 (1999).
11. L. D. Landau and E. M. Lifshitz, *Fluid Mechanics* (Addison–Wesley, Reading, MA, 1959).
12. A. J. C. Ladd, *J. Chem. Phys.* **93**, 3484 (1990).
13. R. Zwanzig and M. Bixon, *Phys. Rev. A* **2**, 2005 (1970).
14. D. Bedeaux and P. Mazur, *Physica* **78**, 505 (1974).
15. M. W. Heemels, A. F. Bakker, and C. P. Lowe, *Prog. Colloid Polym. Sci.* **110**, 150 (1998).
16. J.-P. Hansen and I. R. McDonald, *The Theory of Simple Liquids* (Academic Press, London, 1986).
17. C. W. J. Beenakker and P. Mazur, *Physica A* **128**, 48 (1984).